

Received March 14, 2020, accepted March 25, 2020, date of publication March 30, 2020, date of current version April 22, 2020.

Digital Object Identifier 10.1109/ACCESS.2020.2984263

Multimedia Image Compression Method Based on Biorthogonal Wavelet and Edge Intelligent Analysis

TAO LIU¹ AND YALIN WU^{2,3}

¹College of Information Science and Technology, Zhengzhou Normal University, Zhengzhou 450044, China

²Department of Smart Media, Jeonju University, Jeonju 560759, South Korea

³School of Information Engineering, Jiangxi Software Vocational University of Technology, Nanchang 330041, China

Corresponding author: Yalin Wu (wuyalinvr@163.com)

This work was supported by the National Nature Science Foundation of China under Grant 61572447.


ABSTRACT At present, network image communication is still restricted by channel coding, image and multimedia transmission and other key technologies. Therefore, the transmission process needs to convert the image signal into a digital signal, and then use the relevant band compression technology to reduce these signals to narrow the occupied frequency band, that is, to reduce the amount of information to be transmitted in synchronous transmission. Wavelet transform is a powerful tool for image compression because of its low entropy, multi-resolution, decorrelation and flexible base selection. In this paper, a method of multimedia image compression based on biorthogonal wavelet packet is proposed, which includes the establishment of linear phase biorthogonal wavelet basis, the selection of 3 or 4 levels of wavelet decomposition and reconstruction stage, and the combination of improved band division and preservation strategy. Finally, a compression test is performed based on the selected wavelet basis function and the optimal decomposition and reconstruction layers of the standard test image, which enables to obtain a more ideal compression ratio.

INDEX TERMS Multimedia image compression, biorthogonal wavelet, multimedia transmission, discrete cosine transform.

I. INTRODUCTION

Artificial intelligence is mostly concentrated in large-scale computing clusters such as cloud computing centers, and the end-to-cloud transmission delay has become a wall of intelligent services [1], [2]. In order to make the intelligence closer to users and better serve people, edge intelligence emerged at the historic moment, that is, combining intelligent technology and edge computing technology, pushing intelligent services from cloud computing centers to edge devices to improve the quality of intelligent services [3], [4]. Although data storage technology has been developing, the performance of computers has been increasing, and the channel transmission bandwidth has been continuously widened, but it still cannot keep up with people's requirements for data compression to reduce physical storage space [5], [6]. More and more people have higher requirements for changing demand for channel utilization. The current multimedia image communication transmission technology enables large-capacity data

transmission to be implemented in a more flexible manner, and has more options for image compression transmission technology. In order to save network bandwidth resources, some researchers have proposed various methods to reduce data transmission in different environments, which are mainly manifested in edge cloud collaboration and model compression [7], [8]. The reason why wavelets have great advantages in the field of signal processing is that wavelets conversion can obtain a multi-resolution description of the signal, and having a rich wavelet basis to adapt to signals with different characteristics, which has become a powerful tool for analyzing and studying non-stationary signals [9], [10]. The wavelet analysis method used for signal and image compression has a high compression ratio and fast compression speed. After compression, the characteristics of the signal and image are kept unchanged, and it can resist interference during the transmission process [11], [12]. Adaptive filtering and other fields have been widely used, and it is one of the most active applied research fields [13], [14]. This paper studies the relationship between the approximation and balance of biorthogonal wavelets, and uses the lifting format to construct biorthogonal

The associate editor coordinating the review of this manuscript and approving it for publication was Zhihan Lv .

balanced multiwavelets and use them for multimedia image compression to reduce data transmission.

The special contributions of this paper include:

- Edge intelligence and existing wavelet algorithms are reviewed, and their advantages and disadvantages are analyzed.

- Based on the theory of wavelet analysis, this paper introduces the decomposition and reconstruction algorithm of biorthogonal wavelet packet, including wavelet transform and its important properties, multi-resolution analysis method, two-dimensional Mallat fast decomposition and reconstruction algorithm, wavelet packet algorithm, etc.

- This paper discusses several key links in wavelet multimedia image compression, including evaluation of image quality, selection of filters, and determination of decomposition levels, wavelet packet image compression, and boundary problems.

- A biorthogonal balanced multiwavelet is constructed by using lifting scheme for image compression. The linear phase biorthogonal wavelet basis for multimedia image compression is determined from two aspects of smoothness and filter length.

The rest of this paper is organized as follows. Section 2 discusses related work, followed by characteristic analysis of wavelet transform and construction of 2D wavelet transform in Section 3. The multi-media image compression algorithm based on double orthogonal wavelet is discussed in Section 4. Section 5 shows the experimental results, and Section 6 concludes the paper with summary and future research directions.

II. RELATED WORK

Network multimedia image data compression requires collaboration between edges, establishes a secure communication mechanism, enhances data sharing and collaboration capabilities between edge devices, and improves service quality while protecting data privacy [15], [16]. Compared to cloud computing, edge computing sinks computing resources and efficient services to the edge of the network, which has lower latency, lower bandwidth consumption, higher energy efficiency, and better privacy protection. Under the existing technical conditions, in order to achieve fast or real-time processing, transmission, and storage of data and improve communication capabilities, the only solution is to effectively compress and process multimedia data and study how to use the redundancy inherent in the data itself. The technology of irrelevance and irrelevance enables a large file to be decomposed or converted into a smaller data file without losing important information. The purpose of multimedia image compression research is to seek high compression ratio, less distortion during network transmission and recovery process, etc [17], [18]. With the rapid development of information technology, image compression and transmission technology has a broader prospect, and it also brings more immense challenges. For a long time, the traditional discrete cosine transform (DCT) encoding image compression method has shortcomings, such as the compression efficiency of the

image is not high, the compressed image needs to be decomposed into pixel blocks to bring inevitable block effect, and so on [19]. However, with the advent of wavelet conversion, defects such as the square effect described above have been effectively rectified [8]. In the application of multimedia image compression, wavelets maintain energy in orthogonal performance, and symmetry is suitable for the visual system of the human eye, and makes the signal easy to process at the boundary [20], [21]. The filter corresponding to the tightly supported wavelet is a FIR Device. However, wavelet analysis still has many issues as far as image compression is concerned, such as generating large wavelet coefficients way too easily at the image's boundary and so on [22]. Orthogonal wavelets on balanced intervals solve these problems to a certain extent. Biorthogonal wavelet bases have characteristics such as linear phase, large vanishing moment, and appropriate energy concentration [23]. They have a wide range of applications in image processing [24].

From the early 1950s of the last century, the research on image compression coding started. This first generation of research is mainly based on the entropy principle of information theory. This method has relatively low compression efficiency. Therefore, in the subsequent research of image compression coding technology, transformation processing was introduced. The most commonly used is the DCT transformation [25], [26]. It is precisely because the DCT transformation has a moderate complexity and the coding effect of the transformed image is good. Therefore, the DCT transformation is the core transformation algorithm of many international image coding standards [27], [28]. After 1990, the rapid development of multimedia application technology, digital Internet, and mobile communications, and image compression and coding technology suitable for Internet transmission began to be widely used. At the same time, the rapid growth of related marginal disciplines and the continuous emergence of new disciplines have also contributed to image compression. The study of technology has injected new vitality. Combining theories of computer vision, neural network, wavelet analysis, and fractal geometry has become a new approach to image compression algorithm research. With the continuous research on transformation, wavelet transform has been widely studied and applied because of its high compression efficiency, fast compression speed and no interference during transmission. Now the wavelet transform algorithm in image compression coding has become a mainstream direction in the research of image compression coding technology [29]. From a signal processing perspective, as a new time-frequency analysis tool, wavelet overcomes the shortcomings of the Fourier analysis method that can clearly reveal the frequency characteristics of the signal but cannot reflect the local information in the time domain. The description of properties is important both in theory and in practical applications. When using wavelet to perform time-frequency analysis, it has relatively local and time-frequency characteristics and multi-resolution analysis characteristics, which makes it relatively easy to process non-stationary

signals [30]. Even though the short-duration Fourier conversion can partially locate the time, because the window size is fixed, it is only suitable for stationary signals with small frequency fluctuations and not for non-stationary signals with large frequency fluctuations [31], [32]. The wavelet conversion can automatically adjust the window size according to the level of the frequency. It is an adaptive time-frequency analysis method that can perform multi-resolution analysis. Wavelet analysis is a new discipline that has developed rapidly since the foundation work of Y. Meyer, S. Mallat, and I. Daubechies, etc. since 1986. It is the product of the epoch-making development of traditional Fourier analysis. In 1988, Mallat introduced the idea of multi-resolution analysis to wavelet analysis, construction of wavelet functions, decomposition and reconstruction according to wavelet transforms, thereby successfully unifying the construction of specific wavelet functions before that, and giving the general approach to constructing orthogonal wavelets [33]. At the same time, Dr. Daubechies used multi-resolution analysis to construct orthogonal wavelets with limited support. T. chamitchian constructed the first biorthogonal wavelet basis. As a special wavelet, the biorthogonal compactly supported set wavelet can have compact support, high vanishing moment, and symmetry at the same time. Its development process has been accompanied by the development of wavelet, and its construction theory has received extensive attention and research. Biorthogonal wavelet bases with tightly supported sets make wavelet analysis more suitable for signal processing. The lifting format is a bi-orthogonal wavelet construction method based entirely on the time domain. Compared with the spectral decomposition method, the lifting format has a fixed wavelet construction formula. It is not only simple and easy to understand, but also versatile and flexible implementation of wavelet conversion [34], [35].

III. 2D WAVELET TRANSFORM AND ITS FAST ALGORITHM

A. CHARACTERISTIC ANALYSIS OF WAVELET TRANSFORM

Compared with Fourier transform, wavelet analysis is a localized transform of time and frequency, thus can effectively extract information from the signal. It solves many problems that Fourier cannot by conducting multi scale analysis to function or signal through functions such as expansion and translation, etc. The essential difference between the two is that Fourier only considers the one-to-one mapping between time domain and frequency domain, which represents the signal with the function of a single variable. Wavelet analysis fundamentally overcomes the shortcoming of only describing the signal as a single variable by analyzing nonstationary signals with combined time-scale function [36], [37].

Continuous Wavelet Transform (CWT) is defined as follows,

$$W(a, b) = \int_{-\infty}^{\infty} x(t) \frac{1}{\sqrt{a}} \psi\left(\frac{t-b}{a}\right) dt \quad (1)$$

In which, a and b control the two transforms of the wavelet. a can extend the signal in time and change the center frequency of wavelet transform.

Let the center frequency of parent wavelet be “ F_c ”, then equivalent signal frequency (pseudo-frequency) of the sub wavelet is $F_{eq} = F_c/a\Delta_t$ (“ F_c ” is the wavelet center frequency of scale 1, “ a ” is the scale, “delta t ” is the sampling interval) or $F_{eq} = F_c f_s/a$ (“ f_s ” is sampling frequency). The center frequency refers to the frequency of the wavelet transform. The smallest frequency is the frequency of the wavelet, which can represent the frequency of the middle part of the wavelet and the energy of the wavelet [19].

$a = 1$ is the basis wavelet. When $a < 1$, the time domain compresses, the bandwidth increases and the frequency increases. When $a > 1$, the time domain stretches, the bandwidth decreases and the frequency decreases. In fact, the bandwidth is only related to “ a ”, and the time width * frequency width is a constant. The larger the scale, the lower the frequency, the higher the time resolution, the lower the frequency resolution; the smaller the scale, the higher the frequency the lower the time resolution, the higher the frequency resolution. This characteristic is important [38].

The bandwidth and center frequency of the bandpass filter change along with the scaling factor “ a ”. When “ a ” is smaller, the center frequency is larger and the bandwidth becomes wider. When “ a ” is larger, the center frequency becomes smaller and the bandwidth becomes narrower [39]. This characteristic of wavelet transform has important application value for local characteristic analysis of signal $f(t)$. Where the signal changes slowly, it’s mainly low-frequency, and the frequency range is narrow. The band-pass filter of wavelet transform is equivalent to the larger “ a ” case. Conversely, where the signal changes suddenly, it is mainly high-frequency, with a wide frequency range, and the band-pass filter of wavelet transform is equivalent to the smaller “ a ” case. In summary, when the scaling factor changes from small to large, the range of filtering frequency changes from high to low. Therefore, the wavelet transform has a zoom characteristic [40], [41]. Fig. 1 is a structure chart generated by continuous wavelet transform.

B. CONSTRUCTION OF 2D WAVELET TRANSFORM

Let the discrete Fourier transform of sequence $\{q_n\}$ be $\hat{q}(\omega)$, which satisfy the Fourier transform of $\gamma(t) \in l^2(R)$ as follows,

$$\hat{\gamma}\omega = \frac{1}{\sqrt{2}} \hat{q}\left(\frac{\omega}{2}\right) \hat{\phi}\left(\frac{\omega}{2}\right) \quad (2)$$

Define two 2D separable functions as follows,

$$\begin{cases} \varphi^1(x, y) = \varphi(x) \gamma(y) \\ \varphi^2(x, y) = \varphi(x) \gamma(y) \end{cases} \quad (3)$$

Let the discrete Fourier transform of sequence $\{l_n\}$ be $\hat{l}(\omega)$, which satisfy the Fourier transform of $\tilde{\varepsilon}(t) \in l^2(R)$ as

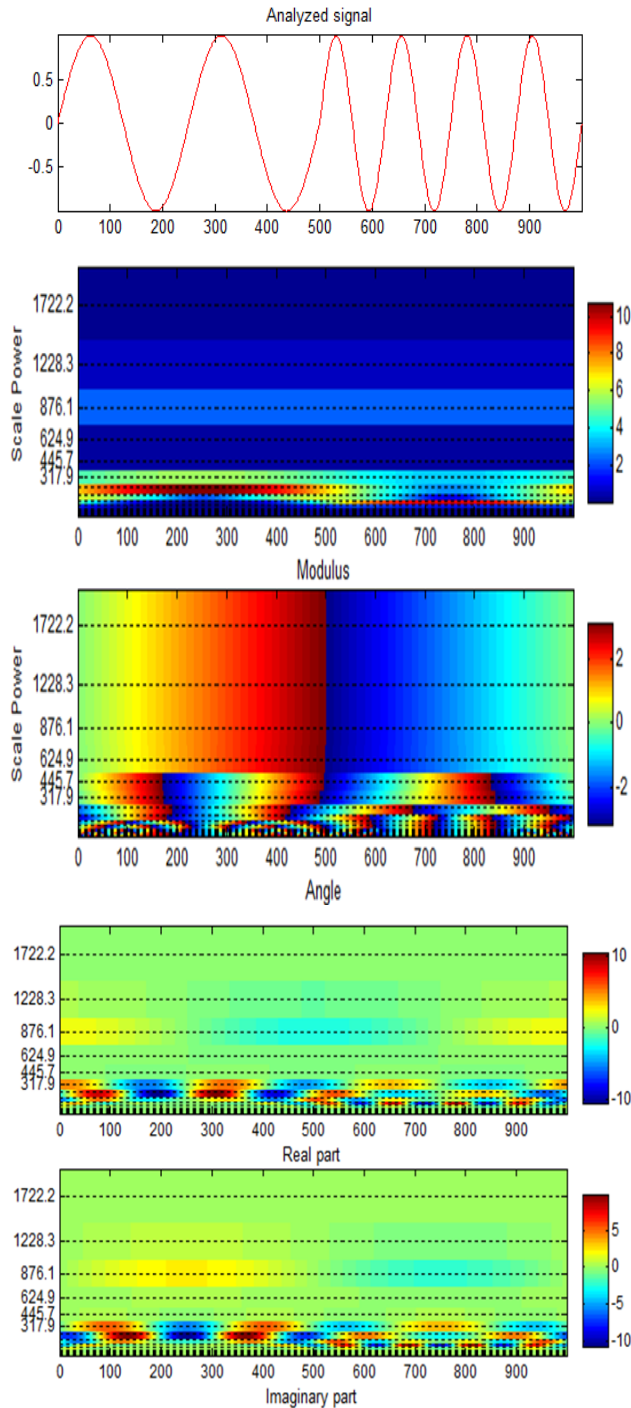


FIGURE 1. Structure chart generated by continuous.

follows,

$$\hat{\varepsilon}(\omega) = \frac{1}{\sqrt{2}} \hat{l}\left(\frac{\omega}{2}\right) \hat{\varphi}\left(\frac{\omega}{2}\right) \quad (4)$$

Define the other two 2D separable functions $\tilde{\varphi}^1(x, y)$ and $\tilde{\varphi}^2(x, y)$ as follows,

$$\begin{cases} \tilde{\varphi}^1(x, y) = \tilde{\varphi}(x) \tilde{\varepsilon}(y) \\ \tilde{\varphi}^2(x, y) = \tilde{\varepsilon}(x) \tilde{\varphi}(y) \end{cases} \quad (5)$$

If $\hat{h}(\omega)^2 + \hat{g}(m) \hat{g}^*(\omega) = 2$, and $\hat{q}(\omega) \hat{l}^*(\omega) = 2 + |\hat{h}(\omega)|^2/2$, then $\varphi^1(x, y)$, $\varphi^2(x, y)$ and $\tilde{\varphi}^1(x, y)$, $\tilde{\varphi}^2(x, y)$ must be two-dimensional binary wavelet, and equals to its re-constructural wavelet.

If $g = \tilde{g}$, $\hat{q}(\omega) = \hat{l}(\omega)$, then $\varphi(t) = \tilde{\varphi}(t)$, $\gamma(t) = \tilde{\varepsilon}(t)$, and $\varphi^1(x, y) = \tilde{\varphi}^1(x, y)$, $\varphi^2(x, y) = \tilde{\varphi}^2(x, y)$. In this case, $\varphi^1(x, y)$, $\varphi^2(x, y)$ must be two-dimensional binary wavelet, and equals to its re-constructural wavelet.

$$|\hat{l}(\omega)|^2 = \frac{2 + |\hat{h}(\omega)|^2}{2} \quad (6)$$

Especially, when $\hat{h}(\omega) = \sqrt{2} \sqrt{\hat{\varphi}_m(2\omega)/\hat{\varphi}_m(\omega)} = \sqrt{2} [\cos \omega/2]^{m+1} e^{-i\omega/2}$, then

$$|\hat{l}(\omega)|^2 = 1 + \left(\cos \frac{\omega}{2}\right)^{2m+2} \quad (7)$$

Let

$$\hat{l}(\omega) = \left(\frac{2 + |\hat{h}(\omega)|^2}{2}\right)^{1/2} \quad (8)$$

Then

$$l_n = \frac{1}{2\pi} \int_{-\pi}^{\pi} \hat{l}(\omega) e^{in\omega} d\omega \quad (9)$$

Wavelet transform basis has both frequency local property and time local property. The multi-resolution transform of wavelet transform can be decomposed on multiple scales, and it is convenient to observe the characteristics of signal at different scales (resolution) at different times. Using wavelet for compression, after wavelet transform, the statistical characteristics are improved to eliminate the correlation between rows and columns [42]. Wavelet bases (scale function and wavelet function) can be generated by given filter coefficients. Some wavelet bases are orthogonal and some are non-orthogonal. Some are symmetrical, and some are asymmetrical. The approximate coefficient and detail coefficient of wavelet can be directly derived by filtering coefficient, without the need to know the wavelet basis function exactly, so that the calculation is simplified, which is the basis of wavelet decomposition and reconstruction [43].

After wavelet decomposition, a series of sub-images with different resolution can be obtained, and sub-images with different resolution have different frequencies. Most of the points on high-resolution (i.e., high-frequency) sub-images are close to 0. The higher the resolution, the more obvious the phenomenon is. It should be noted that in N-level 2D wavelet decomposition, the higher the decomposition level of sub-image, the lower the frequency. Fig. 2 is coefficient value of db3 wavelet continuous transform with different scales.

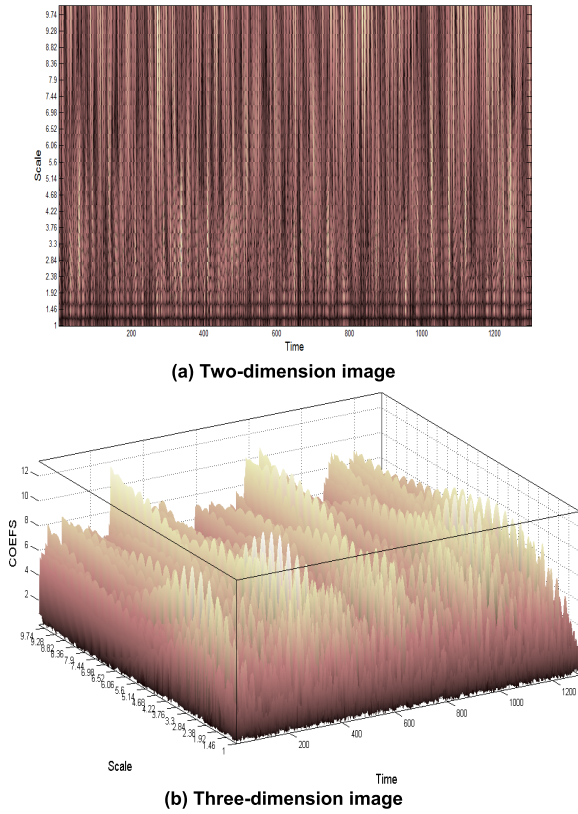


FIGURE 2. Coefficient value of db3 wavelet continuous transform with different scales.

IV. REALIZATION OF MULTI-MEDIA IMAGE COMPRESSION BASED ON DOUBLE ORTHOGONAL WAVELET

A. CONSTRUCTION OF DOUBLE ORTHOGONAL WAVELET

The discrete wavelet transform of $x(t)$ is

$$WT_x(j, k) = \int x(t) \psi_{j,k}(t) dt = \langle x(t), \psi_{j,k}(t) \rangle, \quad j, k \in Z \quad (10)$$

Let $d_j(k) = WT_x(j, k)$, then $d_j(k)$ is called wavelet coefficient, that is the DWT of $x(t)$. Re-construct $x(t)$ with $d_j(k)$ can get,

$$\begin{aligned} x(t) &= \sum_{j=0}^{\infty} \sum_{k=-\infty}^{\infty} d_j(k) \hat{\psi}_{j,k}(t) \\ &= \sum_{j=0}^{\infty} \sum_{k=-\infty}^{\infty} \langle x(t), \psi_{j,k}(t) \rangle \hat{\psi}_{j,k}(t) \end{aligned} \quad (11)$$

In which, $\hat{\psi}_{j,k}(t)$ is the dual wavelet of $\psi_{j,k}(t)$. It can be seen that, wavelet $\psi_{j,k}(t)$ is used for signal analysis while dual wavelet $\hat{\psi}_{j,k}(t)$ is used for signal synthesis. In the case of orthogonal wavelet, $\hat{\psi}_{j,k}(t) = \psi_{j,k}(t)$.

In the case of a double orthogonal filter set, decomposing filter (H_0, H_1) and re-constructing filter (\hat{H}_0, \hat{H}_1) will generate two scale functions ($\varphi, \hat{\varphi}$) and two wavelet functions ($\psi, \hat{\psi}$). in which, φ and ψ represent the decomposition of

signals, while $\hat{\varphi}$ and $\hat{\psi}$ refer to the re-construct of signals. The relationship between them and $H_0, \hat{H}_0, H_1, \hat{H}_1$ are all follows,

$$\varphi(t) = \sqrt{2} \sum_{n=-\infty}^{\infty} h_0(n) \varphi(2t - n) \quad (12)$$

$$\hat{\varphi}(t) = \sqrt{2} \sum_{n=-\infty}^{\infty} \hat{h}_0(n) \hat{\varphi}(2t - n) \quad (13)$$

$$\psi(t) = \sqrt{2} \sum_{n=-\infty}^{\infty} h_1(n) \varphi(2t - n) \quad (14)$$

$$\hat{\psi}(t) = \sqrt{2} \sum_{n=-\infty}^{\infty} \hat{h}_1(n) \hat{\varphi}(2t - n) \quad (15)$$

And

$$\Phi(2\omega) = \frac{1}{\sqrt{2}} H_0(\omega) \Phi(\omega) \quad (16)$$

$$\hat{\Phi}(2\omega) = \frac{1}{\sqrt{2}} \hat{H}_0(\omega) \hat{\Phi}(\omega) \quad (17)$$

$$\Psi(2\omega) = \frac{1}{\sqrt{2}} H_1(\omega) \Phi(\omega) \quad (18)$$

$$\hat{\Psi}(2\omega) = \frac{1}{\sqrt{2}} \hat{H}_1(\omega) \hat{\Phi}(\omega) \quad (19)$$

The relationship between orthogonal filter sets $H_0(\omega)$ and $H_1(\omega)$ is as follows,

$$H_0^*(\omega) \hat{H}_0(\omega) + H_0^*(\omega + \pi) \hat{H}_0(\omega + \pi) = 2 \quad (20)$$

Let $l = 0$, then the relationship between the decomposition and re-construct filters are as follows,

$$H_1(z) = z^{-1} \hat{H}_0(-z^{-1}), \quad \text{or } H_1(\omega) = e^{-j\omega} \hat{H}_0^*(\omega + \pi) \quad (21)$$

$$\hat{H}_1(z) = z^{-1} H_0(-z^{-1}), \quad \text{or } \hat{H}_1(\omega) = e^{-j\omega} H_0^*(\omega + \pi) \quad (22)$$

As in orthogonal wavelets, it also requires $\varphi(t)$ and $\hat{\varphi}(t)$ be low pass, $\psi(t)$ and $\hat{\psi}(t)$ be band pass. Correspondingly, it requires $H_0(z)$ and $\hat{H}_0(z)$ be low pass, $H_1(z)$ and $\hat{H}_1(z)$ be high pass, that is,

$$H_0(\omega) = \hat{H}_0(\omega) |_{\omega=\pi} = 0 \quad (23)$$

$$H_1(\omega) = \hat{H}_1(\omega) |_{\omega=0} = 0 \quad (24)$$

$$\int \varphi(t) dt = \int \hat{\varphi}(t) dt = 1 \quad (25)$$

$$\int \psi(t) dt = \int \hat{\psi}(t) dt = 0 \quad (26)$$

Then

$$\begin{aligned} H_0(\omega) \hat{H}_0(\omega) |_{\omega=0} = 2, \quad \text{and } H_0(\omega) = \hat{H}_0(\omega) |_{\omega=0} = \sqrt{2} \\ H_1(\omega) \hat{H}_1(\omega) |_{\omega=\pi} = 2, \quad \text{and } H_1(\omega) = \hat{H}_1(\omega) |_{\omega=\pi} = \sqrt{2} \end{aligned} \quad (27)$$

From formula (16) and (17), below are generated,

$$\Phi(\omega) = \prod_{j=1}^{\infty} \frac{H_0(\omega/2^j)}{\sqrt{2}} \quad (28)$$

$$\hat{\Phi}(\omega) = \prod_{j=1}^{\infty} \frac{\hat{H}_0(\omega/2^j)}{\sqrt{2}} \quad (29)$$

From formula (18) and (19), below are generated,

$$\Psi(\omega) = \frac{H_1(\omega/2)}{\sqrt{2}} \prod_{j=2}^{\infty} \frac{H_0(\omega/2^j)}{\sqrt{2}} \quad (30)$$

$$\hat{\Psi}(\omega) = \frac{\hat{H}_1(\omega/2)}{\sqrt{2}} \prod_{j=2}^{\infty} \frac{\hat{H}_0(\omega/2^j)}{\sqrt{2}} \quad (31)$$

From the above, it can be seen that in the case of double orthogonality, the filter set and the two-scale difference equation each add a set of dual, that is, $H_0, \hat{H}_0; H_1, \hat{H}_1; \Phi, \hat{\Phi}$ and $\Psi, \hat{\Psi}$.

The decomposition equation and the reconstruction equation under the double orthogonal wavelet are as follows:

$$a_j(n) = a_{j-1}(n) * \bar{h}_0(2n) = \sum_{k=-\infty}^{\infty} a_{j-1}(k)h_0(k - 2n) \quad (32)$$

$$d_j(n) = a_{j-1}(n) * \bar{h}_1(2n) = \sum_{k=-\infty}^{\infty} a_{j-1}(k)h_1(k - 2n) \quad (33)$$

$$\begin{aligned} a_{j-1}(n) &= a'_j(n) * \hat{h}_0(n) + d'_j(n) * \hat{h}_1(n) \\ &= \sum_{k=-\infty}^{\infty} a_j(k)\hat{h}_0(n - 2k) + \sum_{k=-\infty}^{\infty} d_j(k)\hat{h}_1(n - 2k) \end{aligned} \quad (34)$$

In which, $a'_j(n), d'_j(n)$ are respectively gained by $a_j(n), d_j(n)$ conducting second interpolation.

B. DETERMINATION OF OPTIMAL BASIS

In a J-layer wavelet packet, the quantity of wavelet packet basis that can be constructed is $2^{4^{J-1}} \leq B_J \leq 2^{\frac{49}{48}4^{J-1}}$. The following methods are selected to construct the optimal wavelet packet basis. Name $M(\{x_k\})$ as cost function, make the smallest basis of the wavelet library as the optimal basis. According to Shannon entropy criterion, we can get $M(x) = -\sum_k p_k \log p_k$, in which, $p_k = \frac{|x_k|^2}{\|x\|_2^2}$, when $p = 0, p \log p = 0$. Since the information entropy is only semi-additive, the addable function $\lambda(x) = -\sum_k |x_k|^2 \lg|x_k|^2$ is introduced, then $M(x)$ can be expressed as,

$$M(x) = \|x\|^2 \lambda(x) + \lg \|x\|^2 \quad (35)$$

In this case, when $\lambda(x)$ is the smallest, $M(x)$ is also the smallest. Here, the cost function is defined by entropy, because under certain mean square error conditions, $\exp M(x)$ is proportional to the quantity of coefficients required to represent the signal. From the point of view of signal processing, using the optimal method to search the optimal base process

is to use as few coefficients as possible to reflect as much information as possible to achieve the purpose of feature extraction.

The double orthogonal wavelet basis is called the optimal double orthogonal wavelet basis when it satisfies that the dimension of wavelet transform matrix M is the minimum matrix, and has the highest order vanishing matrix at the end of the decomposition with one or more free variables to minimize maximum eigenvalue of $A = MM^T$.

C. LIFTING FORMAT OF DOUBLE ORTHOGONAL WAVELET

In general, wavelet does not have to be each other's expansion and translation, but still has the characteristics of the first-generation wavelet, such wavelet is called the second-generation wavelet, which can be constructed through lifting scheme. After the image is decomposed by wavelet, the resolution of its low frequency part is high, and the details of its high frequency part are prominent. The wavelet lifting format is implemented in four ascending and two scaling steps, as follows,

(1) Forecast 1,

$$c_1(2n + 1) = x(2n + 1) + \alpha[x(2n) + x(2n + 2)] \quad (36)$$

(2) Lifting 1,

$$d_1(2n) = x(2n) + \beta[c_1(2n - 1) + c_1(2n + 1)] \quad (37)$$

(3) Forecast 2,

$$c_2(2n + 1) = c_1(2n + 1) + \gamma[d_1(2n) + d_1(2n + 2)] \quad (38)$$

(4) Lifting 2,

$$d_2(2n) = d_1(2n) + \delta[c_1(2n - 1) + c_1(2n + 1)] \quad (39)$$

(5) Coefficient scaling1,

$$c_3(2n + 1) = (1/K) \bullet c_2(2n + 1) \quad (40)$$

(6) Coefficient scaling2,

$$d_3(2n) = K \bullet d_2(2n) \quad (41)$$

In which, $\alpha = -1.586134342, \beta = -0.0529801186, \gamma = 0.1882911075, \delta = 0.443506852, K = 1.230174105$ are the transform operator for the lifting domain of each part.

The following is the decomposition of orthogonal wavelets with two-order vanishing matrix,

$$h(z) = h_0 + h_1z^{-1} + h_2z^{-2} + h_3z^{-3} \quad (42)$$

$$g(z) = -h_3z^2 + h_2z^1 - h_1 + h_0z^{-1} \quad (43)$$

In which,

$$\begin{aligned} h_0 &= \frac{1 + \sqrt{3}}{4\sqrt{2}}, & h_1 &= \frac{3 + \sqrt{3}}{4\sqrt{2}}, \\ h_2 &= \frac{3 - \sqrt{3}}{4\sqrt{2}}, & h_3 &= \frac{1 - \sqrt{3}}{4\sqrt{2}} \end{aligned} \quad (44)$$

the multiphase matrix is

$$P(z) = \tilde{P}(z) = \begin{bmatrix} h_0 + h_2z^{-1} & -h_3z^1 - h_1 \\ h_1 + h_3z^{-1} & h_2z^1 + h_0 \end{bmatrix} \quad (45)$$

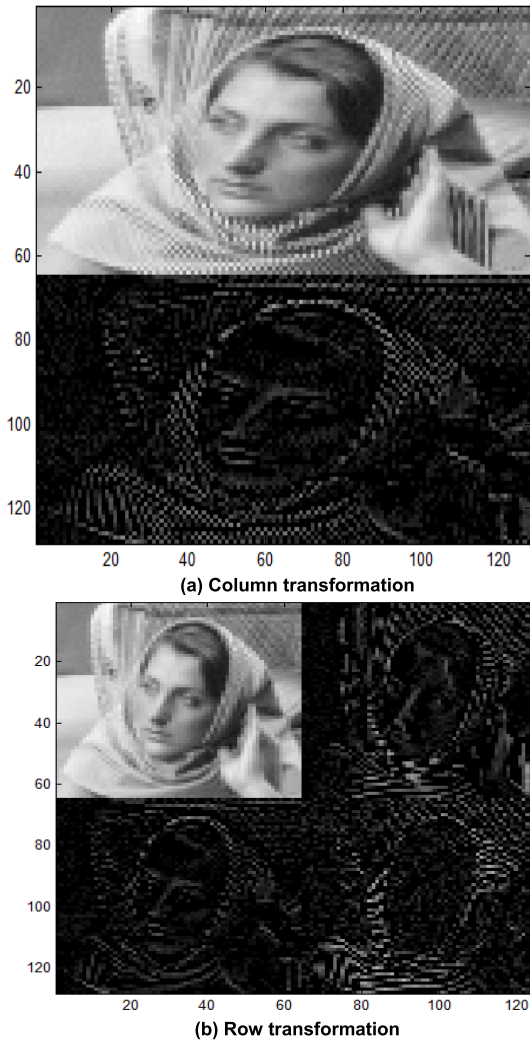


FIGURE 3. Wavelet transform of Woman2 image based on lifting scheme.

the factorization is

$$\begin{aligned}
 P(z) &= \tilde{P}(z) \\
 &= \begin{bmatrix} 1 & -\sqrt{3} \\ 0 & 1 \end{bmatrix} \begin{bmatrix} \frac{\sqrt{3}}{4} + \frac{1}{4}z^{-1} & 0 \\ \frac{\sqrt{3}-2}{4}z^{-1} & 1 \end{bmatrix} \begin{bmatrix} 1 & z \\ 0 & 1 \end{bmatrix} \\
 &\quad \times \begin{bmatrix} \frac{\sqrt{3}+1}{\sqrt{2}} & 0 \\ 0 & \frac{\sqrt{3}-1}{\sqrt{2}} \end{bmatrix} \quad (46)
 \end{aligned}$$

Using Formula (46) as the decomposition of $P(z)$, and the multiphase matrix for analysis is

$$\tilde{P}(1/z)^t = \begin{bmatrix} \frac{\sqrt{3}+1}{\sqrt{2}} & 0 \\ 0 & \frac{\sqrt{3}-1}{\sqrt{2}} \end{bmatrix} \begin{bmatrix} 1 & 0 \\ z^{-1} & 1 \end{bmatrix}$$

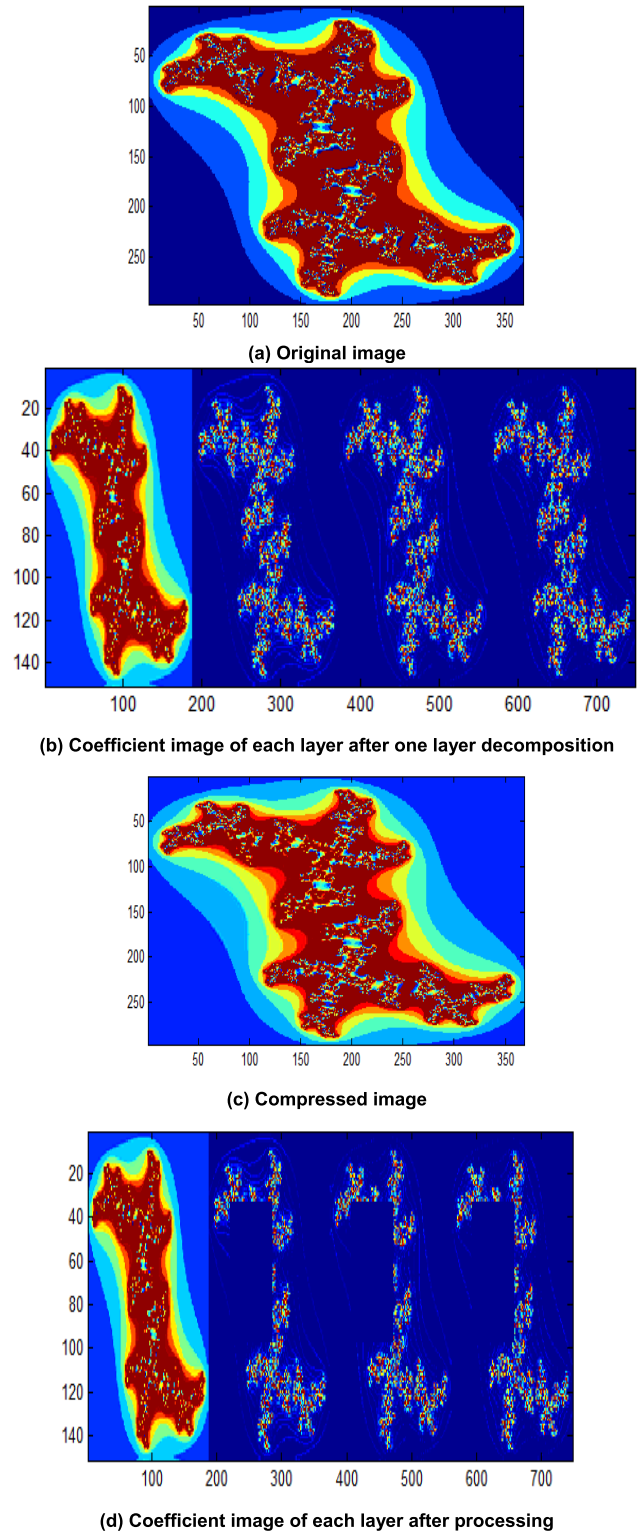


FIGURE 4. Local compression of Julia image using the algorithm proposed in this paper.

$$\times \begin{bmatrix} 1 & \frac{\sqrt{3}}{4} + \frac{\sqrt{3}-2}{4}z \end{bmatrix} \begin{bmatrix} 1 & 0 \\ -\sqrt{3} & 1 \end{bmatrix} \quad (47)$$

the wavelet decomposition algorithm can be obtained as follows,

$$\begin{aligned}
 d_l^{(1)} &= x_{2l+1} - \sqrt{3}x_{2l} \\
 s_l^{(1)} &= x_{2l} + \sqrt{3}/4d_l^{(1)} + (\sqrt{3} - 2)/4d_{l+1}^{(1)} \\
 d_l^{(2)} &= d_l^{(1)} + s_{l-1}^{(1)} \\
 s_l &= (\sqrt{3} + 1)/\sqrt{2}s_l^{(1)} \\
 d_l &= (\sqrt{3} - 1)/\sqrt{2}d_l^{(2)}
 \end{aligned} \tag{48}$$

The reconstruction algorithm can be gained by reversely operating and changing the corresponding symbol of the decomposition algorithm.

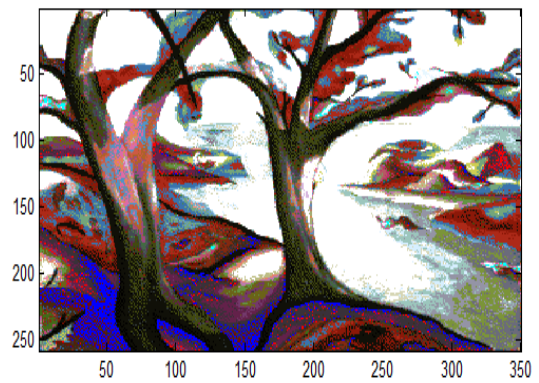
$$\begin{aligned}
 d_l^{(2)} &= (\sqrt{3} + 1)/\sqrt{2}d_l \\
 s_l^{(1)} &= (\sqrt{3} - 1)/\sqrt{2}s_l \\
 d_l^{(1)} &= d_l^{(2)} - s_{l-1}^{(1)} \\
 x_{2l} &= s_l^{(1)} - \sqrt{3}/4d_l^{(1)} - (\sqrt{3} - 2)/4d_{l+1}^{(1)} \\
 x_{2l+1} &= d_l^{(1)} + \sqrt{3}x_{2l}
 \end{aligned} \tag{49}$$

Using lifting scheme for wavelet transform has the advantage of simultaneous address operation, which can save a lot of memory cost. This advantage is more obvious in image processing. Another advantage is that it can improve the speed of wavelet transform. Therefore, decomposing the existing finite-length wavelet filter into basic lifting steps can speed up the wavelet transform. Under the same hardware condition, the operation time is reduced by half for one-dimensional wavelet transform and one-quarter for two-dimensional wavelet transform. This advantage is of great practical value in situations with high real-time requirements. Fig. 3 is wavelet transform of Woman2 image based on lifting scheme.

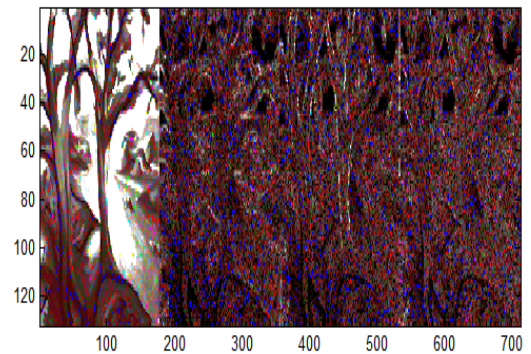
V. TEST EXPERIMENTS AND ANALYSIS

A. SUBJECTIVE EFFECT ANALYSIS OF TEST

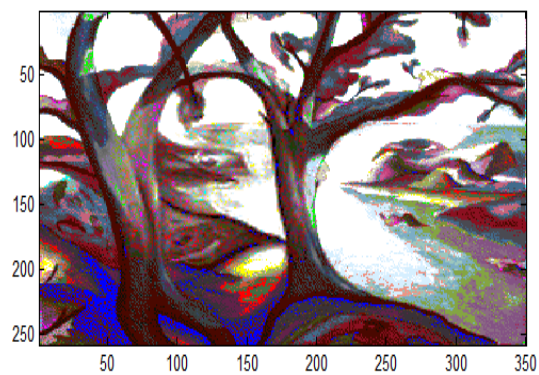
In this paper, the basic idea of double orthogonal wavelet for multimedia image compression is to decompose the image into sub-images with different space and frequency, and then encode the sub-image coefficients. The energy of the image is mainly concentrated in the low frequency part. The horizontal, vertical, and diagonal parts characterize the edge information of the original image, and possess obvious directional characteristics. The low-frequency part can be called as brightness image. Most of the values on the high-resolution sub-image are close to 0, and the higher the resolution, the more obvious this phenomenon is. The most important part to express the image is the low-frequency part, and the wavelet decomposition just is used to remove the high-frequency part and retain the low-frequency one. Fig.4 and Fig. 5 are local wavelet compression processing of Julia and Tree standard test images. Figs. 6-7 are the subjective effect of



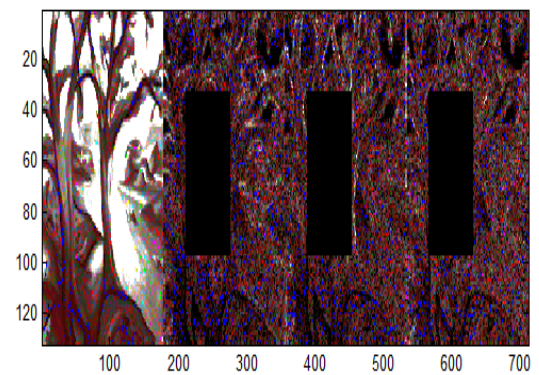
(a) Original image



(b) Coefficient image of each layer after one layer decomposition



(c) Compressed image



(d) Coefficient image of each layer after processing

FIGURE 5. Local compression of Tree image using the algorithm proposed in this paper.

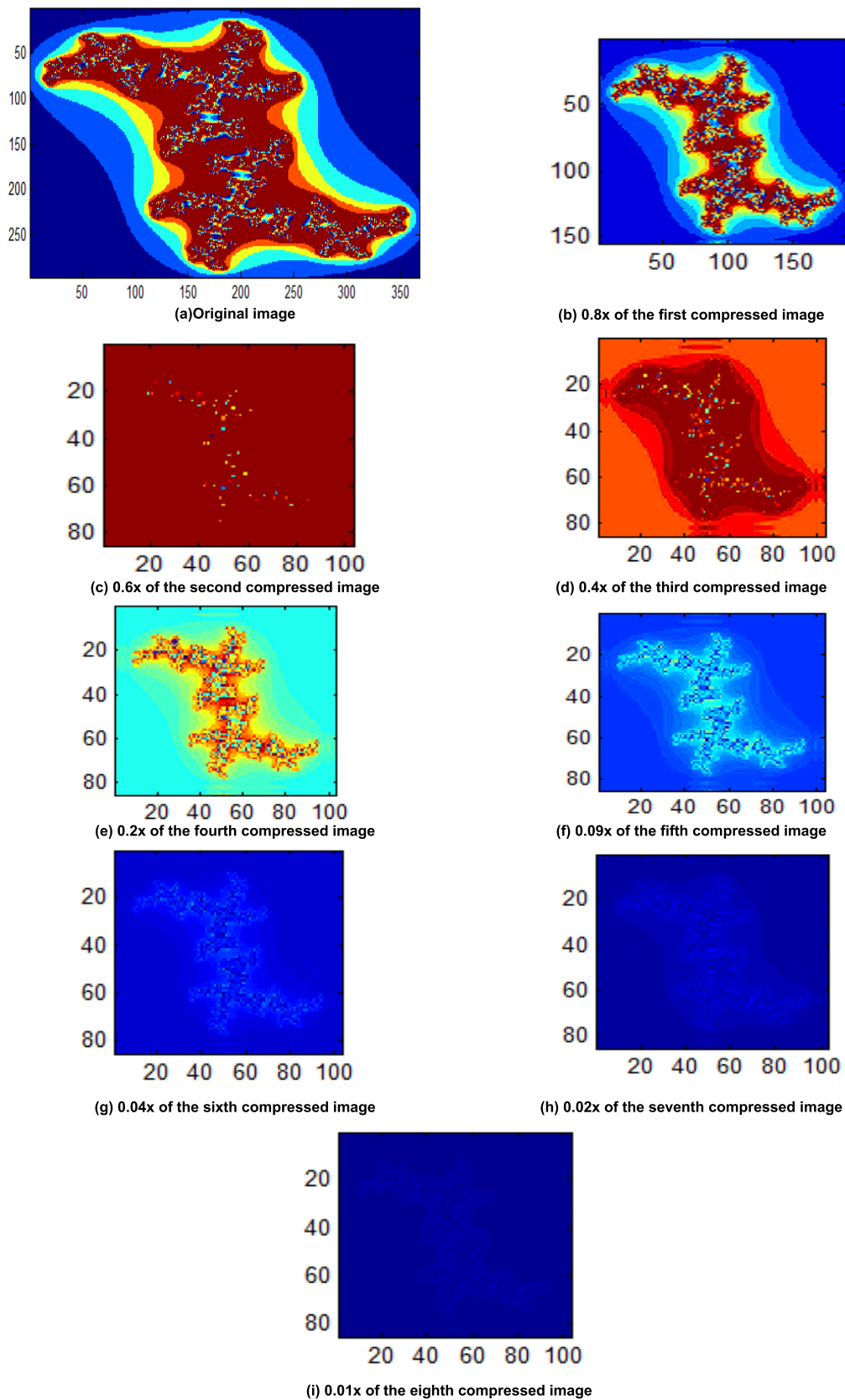


FIGURE 6. Compression of Julia image using the algorithm proposed in this paper.

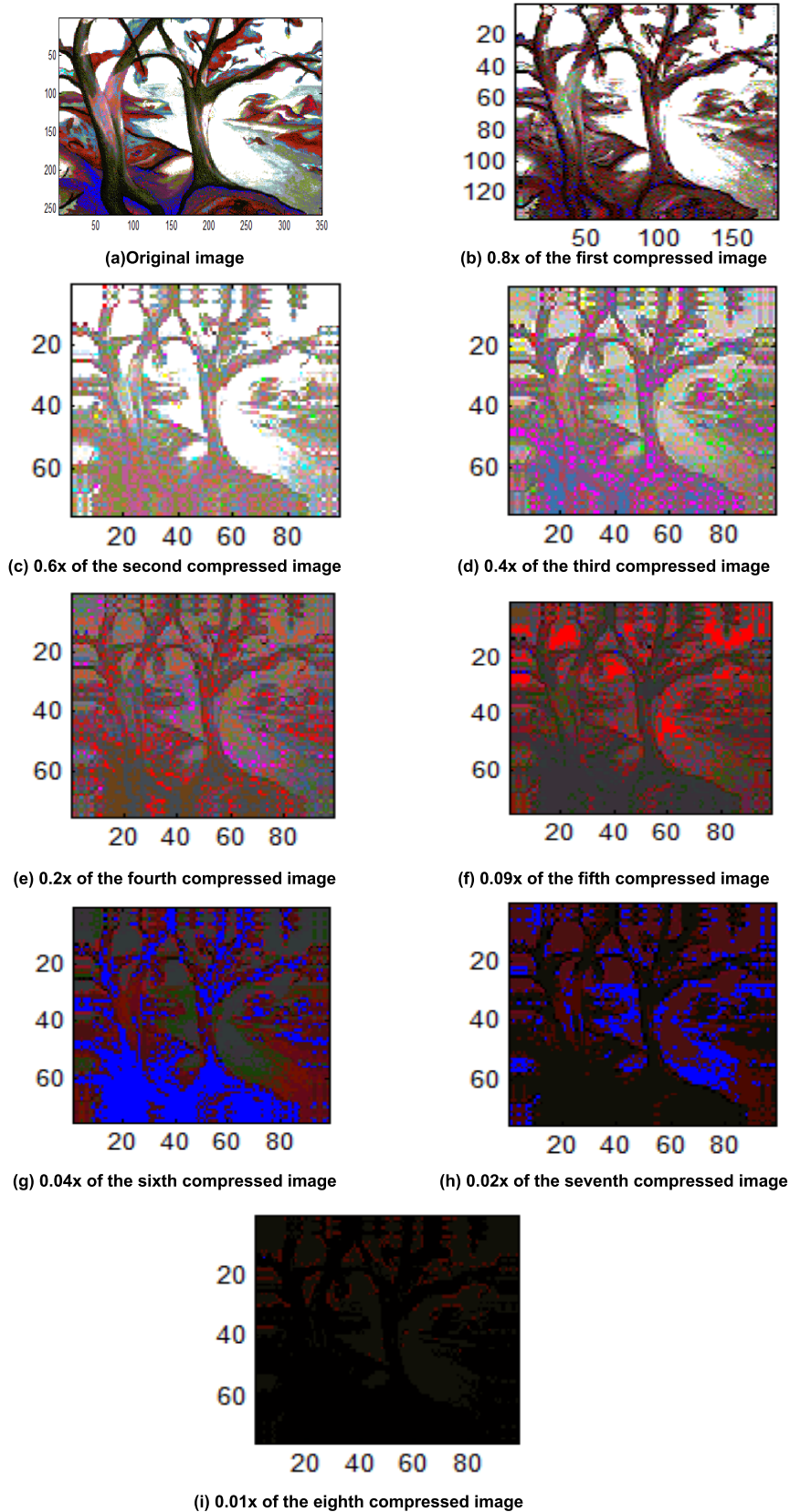


FIGURE 7. Compression of Tree image using the algorithm proposed in this paper.

TABLE 1. PSNR of Lena standard test image compression.

Bit/ Pixel	Algorithm of this paper (dB)	Lena image SPIHT without arithmetic code (dB)	SPIHT with arithmetic code (dB)
0.08	23.67	22.81	23.03
0.125	24.32	23.65	23.94
0.25	25.85	24.93	25.15
0.5	28.13	27.24	27.69
1	32.28	31.47	31.88
2	39.46	38.52	38.97
4	49.85	48.73	49.26

TABLE 2. PSNR of Cameraman standard test image compression.

Bit/ Pixel	Algorithm of this paper (dB)	Camerama image SPIHT without arithmetic code (dB)	SPIHT with arithmetic code (dB)
0.08	29.37	28.66	28.90
0.125	31.21	30.02	30.34
0.25	34.10	33.15	33.48
0.5	37.22	36.24	36.52
1	40.43	39.48	39.75
2	45.08	43.64	44.07
4	55.85	53.03	53.64

the wavelet compression processing of Julia and Tree images using the algorithm proposed in this paper.

In implementation, the discrete filter used by wavelet transform should not be too long, otherwise it will affect the effect of image compression. In order to deal with the boundary problem properly, image wavelet decomposition should not be too frequent, because the more frequent, the more obvious the influence of boundary problem will be. In image compression, the vanishing matrix of the filter is very important. In general, when the tight support set is relatively short, the vanishing matrix of the wavelet filter at the decomposition end should be as high as possible, but the vanishing matrix of the reconstructed end wavelet filter can be relatively low.

B. OBJECTIVE EFFECT ANALYSIS OF TEST

In this paper, the simulation experiment of compression perception reconstruction is carried out with international standard images such as Lena and Cameraman of size 256×256 . To eliminate the randomness of the experiment, the result is averaged 100 times at the same sampling rate. PSNR was used as the evaluation index of image quality. The simulation experiment running environment is matlab, R2014a. the hardware condition is the computer with running 4G memory size and 3.2 GHz CPU.

From Table 1 and Table 2, the following conclusions can be obtained, for standard test images, the PSNR of this paper's algorithm is about 0.3 dB \sim 0.9 dB better than that of PSNR with arithmetic code SPIHT. PSNR with arithmetic code SPIHT is about 0.2 dB \sim 0.6 dB better than PSNR without arithmetic code. The above results illustrate the effectiveness of the double orthogonal wavelet algorithm. The experimental results show that the method adopted in this paper is better than the traditional method in reconstructing the image

quality under the same compression ratio. The compression ratio of this method is about 0.5 times higher than that of the traditional method, and the human visual quality of the reconstructed image is comparable to that of the traditional method. In addition, the proposed compression method has the characteristics of small storage and simple algorithm, which is suitable for hardware implementation and convenient for parallel processing. If the compression algorithm is implemented by DSP, it can further improve the compression speed and realize the real-time compression of multimedia image data in the case of network transmission.

VI. CONCLUSION

Image compression represents the image data with the least number of characters without losing the original information, reducing the space occupied by the information. The goal is ultimately to enable faster and more efficient transmission of various image data to facilitate the next processing step. Because edge intelligence is achieved through preprocessing by network edge devices, the edge device can process data with less time and speed, and can provide certain local and offline service when faced with less computational task requests. The wavelet transform can not only remove the correlation in the image data, but also provides a good mechanism for utilizing the visual characteristics of the human eye. The biorthogonal wavelet is particularly suitable for detecting discontinuous points and lines of complex texture images. In combination with edge intelligence methods, it can also improve the quality of compressed images in multimedia transmission. In this paper, the selected orthogonal wavelet basis and the determined number of decomposition layers are used for compression testing and comparative analysis of standard images. The experimental results show that using this method for multimedia image compression can not only greatly increase the compression ratio, but also obtain better reconstruction results.

REFERENCES

- [1] T. Mahmood, Z. Mehmood, M. Shah, and T. Saba, "A robust technique for copy-move forgery detection and localization in digital images via stationary wavelet and discrete cosine transform," *J. Vis. Commun. Image Represent.*, vol. 53, pp. 202–214, May 2018.
- [2] H. B. Kekre, P. Natu, and T. Sarode, "Color image compression using vector quantization and hybrid wavelet transform," *Procedia Comput. Sci.*, vol. 89, pp. 778–784, Jan. 2016.
- [3] H. Flórez and M. Argáez, "A model-order reduction method based on wavelets and POD to solve nonlinear transient and steady-state continuation problems," *Appl. Math. Model.*, vol. 53, pp. 12–31, Jan. 2018.
- [4] A. Vaish, S. Gautam, and M. Kumar, "A wavelet based approach for simultaneous compression and encryption of fused images," *J. King Saud Univ.-Comput. Inf. Sci.*, vol. 31, no. 2, pp. 208–217, Apr. 2019.
- [5] H. Kusotogullari and A. Yavariabdi, "Evolutionary multiobjective multiple description wavelet based image coding in the presence of mixed noise in images," *Appl. Soft Comput.*, vol. 73, pp. 1039–1052, Dec. 2018.
- [6] Z. Huang, X. Xu, H. Zhu, and M. Zhou, "An efficient group recommendation model with multiattention-based neural networks," *IEEE Trans. Neural Netw. Learn. Syst.*, early access, Jan. 15, 2020, doi: [10.1109/TNNLS.2019.2955567](https://doi.org/10.1109/TNNLS.2019.2955567).
- [7] T. Brahimi, F. Laouir, L. Boubchir, and A. Ali-Chérif, "An improved wavelet-based image coder for embedded greyscale and colour image compression," *AEU-Int. J. Electron. Commun.*, vol. 73, pp. 183–192, Mar. 2017.

- [8] R. Dass, "Speckle noise reduction of ultrasound images using BFO cascaded with Wiener filter and discrete wavelet transform in homomorphic region," *Procedia Comput. Sci.*, vol. 132, pp. 1543–1551, Jan. 2018.
- [9] M. N. Amin, M. A. Rushdi, R. N. Marzaban, A. Yosry, K. Kim, and A. M. Mahmoud, "Wavelet-based computationally-efficient computer-aided characterization of liver steatosis using conventional B-mode ultrasound images," *Biomed. Signal Process. Control*, vol. 52, pp. 84–96, Jul. 2019.
- [10] M. J. Barani, M. Y. Valandar, and P. Ayubi, "A new digital image tamper detection algorithm based on integer wavelet transform and secured by encrypted authentication sequence with 3D quantum map," *Optik*, vol. 187, pp. 205–222, Jun. 2019.
- [11] B. Wu, L. Zong, X. Yan, and C. G. Soares, "Incorporating evidential reasoning and TOPSIS into group decision-making under uncertainty for handling ship without command," *Ocean Eng.*, vol. 164, pp. 590–603, Sep. 2018.
- [12] A. Choudhary and R. Vig, "Face recognition using multiresolution hybrid kekre-DCT wavelet transform features with multiclass ECOC framework," *Procedia Comput. Sci.*, vol. 132, pp. 1781–1787, Jan. 2018.
- [13] R. A. Alotaibi and L. A. Elrefaie, "Text-image watermarking based on integer wavelet transform (IWT) and discrete cosine transform (DCT)," *Appl. Comput. Inform.*, vol. 15, no. 2, pp. 191–202, Jul. 2019.
- [14] G. Zhang, J. Wang, C. Yan, and S. Wang, "Application research of image compression and wireless network traffic video streaming," *J. Vis. Commun. Image Represent.*, vol. 59, pp. 168–175, Feb. 2019.
- [15] M. Budninskiy, H. Owahdi, and M. Desbrun, "Operator-adapted wavelets for finite-element differential forms," *J. Comput. Phys.*, vol. 388, pp. 144–177, Jul. 2019.
- [16] J. C. Galan-Hernandez, V. Alarcon-Aquino, O. Starostenko, J. M. Ramirez-Cortes, and P. Gomez-Gil, "Wavelet-based frame video coding algorithms using fovea and SPECK," *Eng. Appl. Artif. Intell.*, vol. 69, pp. 127–136, Mar. 2018.
- [17] K. B. Sowmya and J. A. Mathew, "Discrete wavelet transform based on coextensive distributive computation on FPGA," *Mater. Today, Proc.*, vol. 5, no. 4, pp. 10860–10866, 2018.
- [18] W. Wei, J. Su, H. Song, H. Wang, and X. Fan, "CDMA-based anti-collision algorithm for EPC global c1 Gen2 systems," *Telecommun. Syst.*, vol. 67, no. 1, pp. 63–71, Jan. 2018.
- [19] G. Priyadarshi and B. V. Rathish Kumar, "Wavelet Galerkin method for fourth order linear and nonlinear differential equations," *Appl. Math. Comput.*, vol. 327, pp. 8–21, Jun. 2018.
- [20] H. Rabbouch and F. Saâdaoui, "A wavelet-assisted subband denoising for tomographic image reconstruction," *J. Vis. Commun. Image Represent.*, vol. 55, pp. 115–130, Aug. 2018.
- [21] F. A. B. Hamzah, T. Yoshida, and M. Iwahashi, "Non-separable four-dimensional integer wavelet transform with reduced rounding noise," *Signal Process., Image Commun.*, vol. 58, pp. 123–133, Oct. 2017.
- [22] K. Mahato, "The composition of fractional Hankel wavelet transform on some function spaces," *Appl. Math. Comput.*, vol. 337, pp. 76–86, Nov. 2018.
- [23] J. Chi and M. Eramian, "Enhancing textural differences using wavelet-based texture characteristics morphological component analysis: A preprocessing method for improving image segmentation," *Comput. Vis. Image Understand.*, vol. 158, pp. 49–61, May 2017.
- [24] K. Hayat and T. Qazi, "Forgery detection in digital images via discrete wavelet and discrete cosine transforms," *Comput. Electr. Eng.*, vol. 62, pp. 448–458, Aug. 2017.
- [25] T. V. N. Prabhakar and P. Geetha, "Two-dimensional empirical wavelet transform based supervised hyperspectral image classification," *ISPRS J. Photogramm. Remote Sens.*, vol. 133, pp. 37–45, Nov. 2017.
- [26] W. Wei, X. Fan, H. Song, X. Fan, and J. Yang, "Imperfect information dynamic stackelberg game based resource allocation using hidden Markov for cloud computing," *IEEE Trans. Services Comput.*, vol. 11, no. 1, pp. 78–89, Jan. 2018.
- [27] M. Hamdi, R. Rhouma, and S. Belghith, "A selective compression-encryption of images based on SPIHT coding and chirikov standard map," *Signal Process.*, vol. 131, pp. 514–526, Feb. 2017.
- [28] N. M. Makbol, B. E. Khoo, T. H. Rassem, and K. Loukhoukha, "A new reliable optimized image watermarking scheme based on the integer wavelet transform and singular value decomposition for copyright protection," *Inf. Sci.*, vol. 417, pp. 381–400, Nov. 2017.
- [29] T. Dolenko, A. Efitorov, O. Sarmanova, O. Kotova, I. Isaev, K. Laptinskiy, S. Dolenko, and S. Burikov, "Application of wavelet neural networks for monitoring of extraction of carbon multi-functional medical nano-agents from the body," *Procedia Comput. Sci.*, vol. 145, pp. 177–183, Jan. 2018.
- [30] M. Sharma, A. A. Bhurane, and U. R. Acharya, "MMSFL-OWFB: A novel class of orthogonal wavelet filters for epileptic seizure detection," *Knowl.-Based Syst.*, vol. 160, pp. 265–277, Nov. 2018.
- [31] Z. Chen, H. Cai, Y. Zhang, C. Wu, M. Mu, Z. Li, and M. A. Sotelo, "A novel sparse representation model for pedestrian abnormal trajectory understanding," *Expert Syst. Appl.*, vol. 138, Dec. 2019, Art. no. 112753.
- [32] B. Wu, T. Cheng, T. L. Yip, and Y. Wang, "Fuzzy logic based dynamic decision-making system for intelligent navigation strategy within inland traffic separation schemes," *Ocean Eng.*, vol. 197, Feb. 2020, Art. no. 106909.
- [33] Z. Huang, J. Tang, G. Shan, J. Ni, Y. Chen, and C. Wang, "An efficient passenger-hunting recommendation framework with multitask deep learning," *IEEE Internet Things J.*, vol. 6, no. 5, pp. 7713–7721, Oct. 2019, doi: 10.1109/JIOT.2019.2901759.
- [34] T. Zhou and J. Zhang, "Analysis of commercial truck drivers' potentially dangerous driving behaviors based on 11-month digital tachograph data and multilevel modeling approach," *Accident Anal. Prevention*, vol. 132, Nov. 2019, Art. no. 105256.
- [35] B. Wu, T. L. Yip, X. Yan, and C. G. Soares, "Fuzzy logic based approach for ship-bridge collision alert system," *Ocean Eng.*, vol. 187, Sep. 2019, Art. no. 106152.
- [36] W. Wei, B. Zhou, D. Połap, and M. Woźniak, "A regional adaptive variational PDE model for computed tomography image reconstruction," *Pattern Recognit.*, vol. 92, pp. 64–81, Aug. 2019.
- [37] L. Dong, W. Wu, Q. Guo, M. N. Satpute, T. Znati, and D. Z. Du, "Reliability-aware offloading and allocation in multilevel edge computing system," *IEEE Trans. Rel.*, early access, May 15, 2019, doi: 10.1109/TR.2019.2909279.
- [38] X. Sun, H. Zhang, W. Meng, R. Zhang, K. Li, and T. Peng, "Primary resonance analysis and vibration suppression for the harmonically excited nonlinear suspension system using a pair of symmetric viscoelastic buffers," *Nonlinear Dyn.*, vol. 94, no. 2, pp. 1243–1265, Oct. 2018.
- [39] Y. Wang, E. Zio, X. Wei, D. Zhang, and B. Wu, "A resilience perspective on water transport systems: The case of eastern star," *Int. J. Disaster Risk Reduction*, vol. 33, pp. 343–354, Feb. 2019.
- [40] Z. Huang, X. Xu, J. Ni, H. Zhu, and C. Wang, "Multimodal representation learning for recommendation in Internet of Things," *IEEE Internet Things J.*, vol. 6, no. 6, pp. 10675–10685, Dec. 2019.
- [41] W. W. X. Xia, M. Wozniak, X. Fan, R. Damaševičius, and Y. Li, "Multi-sink distributed power control algorithm for Cyber-physical-systems in coal mine tunnels," *Comput. Netw.*, vol. 161, pp. 210–219, Oct. 2019.
- [42] W. Wei, H. Song, W. Li, P. Shen, and A. Vasilakos, "Gradient-driven parking navigation using a continuous information potential field based on wireless sensor network," *Inf. Sci.*, vol. 408, no. 2, pp. 100–114, 2017.
- [43] L. Dong, Q. Guo, and W. Wu, "Speech corpora subset selection based on time-continuous utterances features," *J. Combinat. Optim.*, vol. 37, no. 4, pp. 1237–1248, May 2019.



TAO LIU received the B.E. degree in computer applications from Information Engineering University, Zhengzhou, China, in 2000, and the M.S. degree in software engineering from Zhengzhou University, Zhengzhou, in 2009.

He is currently an Associate Professor with the School of Information Science and Technology, Zhengzhou Normal University, Zhengzhou. His main research areas include image processing, information security, and network technology.



YALIN WU received the B.E. degree in computer software and the M.S. degree in application software from Dongyi University, Busan, South Korea, in 2008 and 2010, respectively, and the Ph.D. degree in cultural and technological content development from Jeonju University, Jeonju, South Korea, in 2014.

He is currently an Associate Professor with the Department of Smart Media, Jeonju University. His main research areas include image processing, machine learning, and virtual reality.